International Journal of Neuropsychopharmacology (2014), **17**, 1863–1879. © CINP 2014
doi:10.1017/S1461145714000601

ARTICLE

Cumulative effects of the ApoE genotype and gender on the synaptic proteome and oxidative stress in the mouse brain

Lv Shi*, Xin Du*, Hong Zhou, Changlu Tao, Yuntao Liu, Fantao Meng, Gao Wu, Ying Xiong, Chun Xia, Yu Wang, Guoqiang Bi and Jiang-Ning Zhou

CAS Key Laboratory of Brain Function and Diseases, School of Life Science, University of Science and Technology of China, Hefei 230027, Anhui, China

Abstract

Elderly females, particularly those carrying the apolipoprotein E (ApoE)-ε4 allele, have a higher risk of developing Alzheimer's disease (AD). However, the underlying mechanism for this increased susceptibility remains unclear. In this study, we investigated the effects of the ApoE genotype and gender on the proteome of synaptosomes. We isolated synaptosomes and used label-free quantitative proteomics, to report, for the first time, that the synaptosomal proteomic profiles in the cortex of female human-ApoE4 mice exhibited significantly reduced expression of proteins related to energy metabolism, which was accompanied by increased levels of oxidative stress. In addition, we also first demonstrated that the proteomic response in synaptic termini was more susceptible than that in the soma to the adverse effects induced by genders and genotypes. This suggests that synaptic mitochondria might be 'older' than mitochondria in the soma of neurons; therefore, they might contain increased cumulative damage from oxidative stress. Furthermore, female human-ApoE4 mice had much lower oestrogen levels in the cortex and treatment with oestrogen protected ApoE3 stable transfected C6 neurons from oxidative stress. Overall, this study reveals complex ApoE- and gender-dependent effects on synaptic function and also provides a basis for future studies of candidates based on specific pathways involved in the pathogenesis of AD. The lack of oestrogen-mediated protection regulated by the ApoE genotype led to synaptic mitochondrial dysfunction and increased oxidative stress, which might make older females more susceptible to AD.

Received 26 September 2013; Reviewed 28 December 2013; Revised 21 March 2014; Accepted 29 March 2014; First published online 9 May 2014

Key words: Alzheimer's disease, apolipoprotein E, cryo-electron tomography, gender, label-free, oxidative stress, proteomics, synaptosome.

Introduction

The apolipoprotein E (ApoE) ε4 allele is considered to be a risk factor for developing sporadic Alzheimer's disease (AD) (Kim et al., 2009; Chen et al., 2011a). Genome-wide association studies (GWAS) have consistently identified ApoE as an unequivocal susceptibility gene in AD (Avramopoulos, 2009; Harold et al., 2009). ApoE was also strongly associated with the rate of cognitive decline in a GWAS using a quantitative measure of global cognitive decline (De Jager et al., 2012). We demonstrated previously that mild cognitive impairment (MCI) in patients was associated with a higher frequency of the ApoE4 allele. Moreover, there was a significant decline in olfactory identification in MCI subjects bearing the ApoE ε4 allele (Wang et al., 2002). The ApoE 4 carriers with MCI also had significantly reduced cerebral blood flow velocity (Sun et al., 2007).

The presence of one or two ApoE4 alleles has been associated with an increased rate of progression from MCI to AD (Petersen et al., 1995). Numerous studies have revealed that ApoE4 significantly impaired synaptic and mitochondrial function, which might be an early event in the onset of AD. For example, ApoE4 decreased spine density, affected dendritic complexity (Ji et al., 2003; Dumanis et al., 2009), and caused mitochondrial dysfunction (Valla et al., 2010; Chen et al., 2011a) and oxidative damage (Jofre-Monseny et al., 2008) in humans and transgenic mouse models of AD. Greicius and colleagues used functional magnetic resonance imaging, and found weaker brain connectivity in the precuneus and posterior cingulate cortex of female ApoE4 carriers compared with either female ApoE3 homozygotes or male carriers (Damoiseaux et al., 2012). Therefore, there are gender differences in the magnitude of the effect of this allele

Address for correspondence: J.-N. Zhou, Department of Neurobiology and Biophysics, School of Life Science, University of Science and Technology of China, Huangshan Road 443, Hefei, Anhui 230027, China.
Tel.: 0086 -551-3607658 *Fax*: 0086-551-3607778
Email: jnzhou@ustc.edu.cn
* These authors contributed equally to this work.

in the brain. Interestingly, it is generally recognized that elderly females, particularly those carrying ApoE4 allele, have a higher risk of developing AD than males (Payami et al., 1996) and are also more sensitive to the deleterious effects of ApoE4 on cognition (Mortensen and Hogh, 2001).

It is possible that oestrogen deficiency in the brains of post-menopausal females might increase the risk of developing AD (Yue et al., 2005). There is a close relationship between oestrogen and ApoE in the central nervous system (Nathan et al., 2004), where the role of oestrogen in neural protection and synaptic plasticity might be modulated by the ApoE genotype (Stone et al., 1998). In addition, oestrogen replacement therapy (ERT) might reduce the risk of AD in the absence of ApoE4 (Yaffe et al., 2000). However, the ApoE genotype- and gender-specific effects, and the precise molecular alterations that cause cognitive decline in AD, have not been systematically investigated at the synaptic termini. Because synapses constitute the fundamental units of information processing in the brain, synaptic dysfunction is believed to be an underlying mechanism for neurodegenerative diseases such as AD. To study synapse *in vitro*, they are purified into 'synaptosomes', after the mild disruption of brain tissue. This tissue disruption causes nerve terminals to detach from their axons, and the post-synaptic and glial cells to which they were connected, and then reseal to form synaptosomes (Whittaker et al., 1964; Schrimpf et al., 2005; Bayes and Grant, 2009). Previous studies have used this system to identify impaired respiratory capacity in cortical synaptosomes from superoxide dismutase 2(SOD-2) null mice (Flynn et al., 2011). Another study investigated the repair of oxidative DNA base damage in mouse synaptosomes during normal aging and in an AD model (Gredilla et al., 2012).

In this current study, we first examined the specific effects of the ApoE genotype and gender on the synaptic proteome in the mouse brain, using label-free quantitative proteomics. Second, we determined the level of oxidative stress in the cortex of human-ApoE transgenic mice, to confirm if the ApoE4 and female gender risk factor induced changes in protein expression had functional consequences. Third, we measured oestrogen levels and *aromatase* mRNA expression in the cortex of ApoE transgenic mice to further explore the relationship between oestrogen and the ApoE genotype. The protective effect of oestrogen was also assessed in C6 cell stable transfected with different ApoE constructs. Finally, we performed the proteomic profiling in isolated non-synaptic mitochondria in a brain area that was distant from synaptic terminals to assess the effects of ApoE4 genotype and gender.

Method

A brief description of the materials and methods is presented in this section. For a full and detailed description, please refer to the supplementary material.

Animals and treatment

Transgenic mice (Jackson Laboratory, USA) express human ApoE under the control of the human glial fibrillary acidic protein (GFAP) promoter and do not express endogenous mouse ApoE. Mice were maintained on a 12-h light/dark cycle (lights on at 07:00 h), at a temperature of 22±1 °C. Food and water were available *ad libitum*. All procedures were performed according to the Animal Care and Use Committee of University of Science and Technology of China.

Isolation of synaptosomal and non-synaptic mitochondrial fractions

Synaptosomes and non-synaptic mitochondria were isolated using the Percoll (GE Healthcare, Sweden) gradient method with slight modifications (Dunkley et al., 2008; Zhang et al., 2011).

Cryo-electron tomography (Cryo-ET) of the synaptosomes

Synaptosomes embedded in sucrose solution were stored in −80 °C before use. Sucrose was removed by washing with HEPES-buffered saline (HBS) followed by centrifugation for 15 min at 18000 *g* and the pellets were re-suspended in HBS. Four microlitres of sample was mixed with 15 nm gold beads, and added to holey carbon-coated copper grids (Quantifoil Micro Tools, Germany). Extra liquid was absorbed using filter paper, and the grids were then plunged into liquid ethane for rapid vitrification using an FEI Vitrobot (FEI Company, USA).

Data were collected using a Tecnai F20 transmission electron microscope equipped with a FEG and a 4k × 4k CCD camera. The tilt series were aligned and reconstructed using IMOD software (Kremer et al., 1996), and then visualized and segmented with Amira software (TGS, USA).

Trypsin digestion

Fifty microgram protein lysates from the synaptosomes and 20 μg from the non-synaptic mitochondria of each mouse cortex were used. The protein concentration was adjusted to 0.5 μg/μl, and 100 mM DTT was added to a final concentration of 20 mM. All samples were incubated at 37 °C for 2 h, and then 200 mM IAA was added to a final concentration of 40 mM. All samples were incubated for an additional 40 min at room temperature in the dark. Sample were then precipitated with UPPA reagent (Pierce, USA) and centrifuged at 13000 *g* for 20 min at 4 °C. The pellets were solubilized in 100 mM NH_4HCO_3, pH 8.5 and incubated with sequencing-grade trypsin 1:50, w/w, Promega, USA) for 16 h at 37 °C in a shaking incubator.

Mass spectrometry (MS)

For RP-LC MS/MS analysis, 500 and 200 ng protein digests from the synaptosomes and non-synaptic mitochondria were re-dissolved in 0.1% formic acid (FA) in water and loaded onto a Biobasic C18 Picofrit™ column (100 mm length, 75 μm ID) (New Objective, USA). Buffer A (0.1% FA in H_2O) and B (0.1% FA in 100% acetonitrile) were used to generate a gradient from 2 to 98% B in 150 min and were introduced into a linear trap quadrupole (LTQ) ion trap mass spectrometer (Thermo Finnigan, USA) using electrospray ionization from a nanoflow probe at 600 nl/min. The LTQ was set as a full MS scan (m/z 300–2000) followed by four consecutive MS/MS scans of the four most intense ions from the MS spectrum. The electrospray voltage and capillary temperature were 1.8 kV and 200 °C, respectively. To prevent repetitive analysis, dynamic exclusion was enabled with a repeat count of one, a repeat duration of 30 s, and exclusion duration of 60 s. Two blank injections were performed before and after sample analysis to minimize carry-over.

Western blot analysis

Cortex tissues were homogenized in Trizol reagent (Invitrogen, USA) containing cocktail. Proteins were separated on 12% SDS-PAGE gels and then transferred to PVDF membranes. Membranes were blocked in 5% non-fat milk solution and probed with antibodies against cytochrome c oxidase (COX) IV (1:2000, Abcam, USA), SOD2 (1:3000, Abcam, USA), PSD95 (1:1500, Abcam, USA), SYNI (1:3000, Sigma-Aldrich, USA) and β-actin (1:3000, Kangcheng, China). The bands were visualized on X-ray films using ECL reagents (Pierce, USA).

Quantitative determination of glutathione (GSH), glutathione disulfide (GSSG) and malondialdehyde (MDA) levels

GSH and GSSG levels were determined using a protocol described by Rahman et al. (2006). The MDA content in supernatants was determined using kits (Jiancheng, China) and the absorbance was read at 532 nm. All results were expressed as nmol/mg protein.

Oestrogen measurement and aromatase mRNA expression

Mouse 17β-oestradiol (E_2) levels were detected using an enzyme-linked immunosorbent assay kit (Biosource, USA), and the E_2 concentration in the cortex was normalized to total protein. The expression of the ApoE mice *aromatase* gene was calculated using the $2^{-\Delta\Delta Ct}$ method normalized to actin. The efficiency of the primer used was assessed before RT-qPCR measurement.

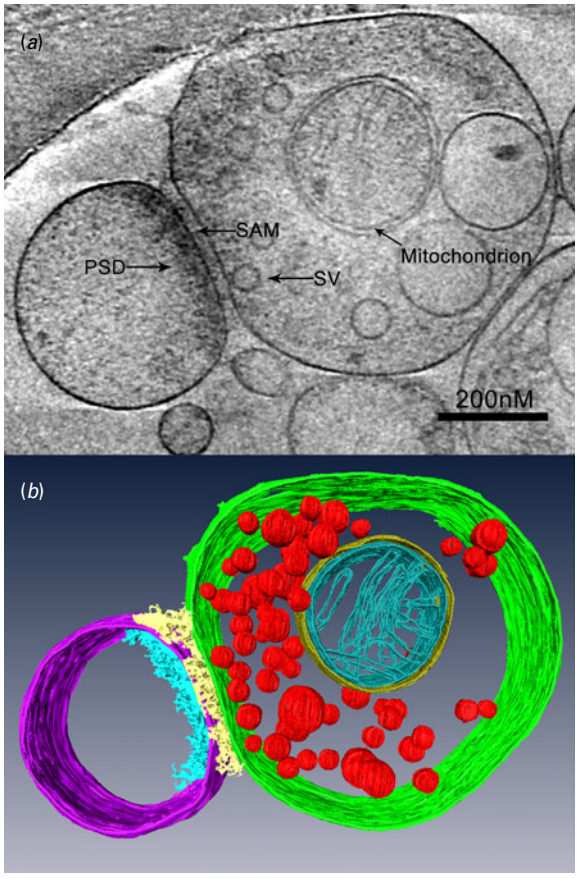

Fig. 1. The sub-cellular distribution of synaptosomes, as assessed by cryo-ET. (*a*) Cryo-ET of the synaptosome shows the structure of the neural terminals: post-synaptic density (PSD), synaptic vesicle (SVs), mitochondria, and synaptic adhesion molecules (SAM). Scale bar = 200 nm. (*b*) The basic configuration was coloured in a 3D rendering of the synaptosome tomogram.

Cell culture and RT-qPCR

ApoE stable transfected C6 cells were cultured in phenol red free Dulbecco's modified Eagle's medium (Sigma-Aldrich, USA), supplemented with 10% charcoal stripped foetal bovine serum (Invitrogen, USA). All cells were cultured at 37 °C in a 5% CO_2-humidified atmosphere. 17β-oestradiol (Sigma-Aldrich, USA) were first dissolved in ethanol and used at a final concentration of 200 nM in 0.01% ethanol. Cultured cells were exposed to H_2O_2 for 24 h. MTT assays were performed to assess cell viability. Expression of the *COXIV* and *SOD2* was calculated using the $2^{-\Delta\Delta Ct}$ method normalized to actin. The efficiency of the primers was assessed before RT-qPCR was performed.

Results

Isolation and cryo-ET imaging of synaptosomes

Synaptosomes have been exhaustively characterized in functional terms, such as the production of ATP and the

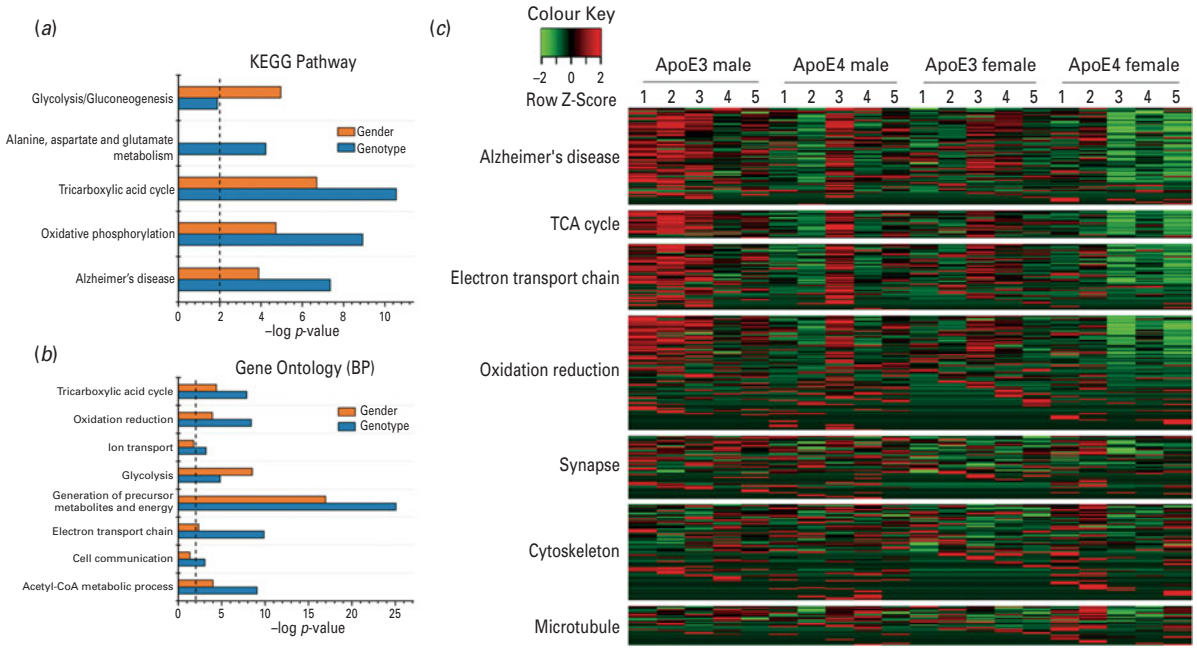

Fig. 2. Proteomic profiling of synaptosomal protein expression. (*a, b*) GO category enrichments of the differentially regulated proteins (genotype- or gender-dependent) based on KEGG pathway and biological processes. GO and pathway analyses were performed using DAVID bioinformatics resources (http://david.abcc.ncifcrf.gov/). Significance is indicated by the *p*-values for each GO category. Process groups were considered significant with at least five protein members and $p<0.05$. The dashed line indicates statistical significance at the $p=0.01$ level. (*c*) Composite heat maps of altered protein abundance were normalized by *z*-score across four groups of mice. The relative *z*-score of 167 proteins from each group mice ($n=5$) is also shown side by side. Green and red colours represent proteins with a lower and higher abundance than the mean. A *z*-score of 0 represents a protein abundance that is equal to the mean of that protein across all samples. Note: significantly decreased pathways (green) converge in the TCA, ETC, oxidation reduction and AD categories in the ApoE4 female group.

release of neurotransmitters (Dunkley et al., 2008). Synaptosomes from the ApoE transgenic mouse cortex were isolated using the Percoll gradient method (Supplementary Figure S1*a*). The enrichment and purity of synaptosomes and non-synaptic mitochondria were confirmed by Western blotting (Supplementary Figure S1*b*). The sub-cellular distribution of synaptosomes was also assessed using the cryo-ET. A 1.5-nm thick virtual section derived from electron tomographic reconstruction displays revealed that the synaptosome, was readily visible, including the structure of nerve terminals, with post-synaptic density, synaptic vesicle (SVs), mitochondrion and synaptic adhesion molecules (Fig. 1*a*). Furthermore, three-dimensional rendering of the same tomogram clearly resolved the basic spatial configuration of the synaptosome (Fig. 1*b*).

ApoE genotype- and gender-dependent alterations in glucose, fatty acids, amino acids and oxidative phosphorylation pathways in the synaptosomal proteome

Enrichment analyses of the Kyoto Encyclopaedia of Genes and Genomes (KEGG) pathways (Fig. 2*a*) and Gene Ontology (GO) biological processes (Fig. 2*b*) showed that the differentially expressed proteins induced by the ApoE genotype or gender risk factor were significantly enriched in signalling pathways linked to metabolism, such as glycolysis, the TCA cycle, amino acid metabolism and oxidative phosphorylation. Heat maps display 167 different proteins and their relative abundance side by side, with a focus on proteins related to energy metabolism, oxidative reduction, synaptic transmission and cytoskeleton (Fig. 2*c*). Interestingly, 81 of the 1043 synaptosomal proteins detected in all 20 mice were significantly affected by ApoE genotype, gender, or both (Table 1, Fig. 2). Of these 81 proteins, 53 (65.4%) were significantly different between ApoE genotypes, 44 (54.3%) differed with genders, and 19 (23.5%) were significantly affected by both variables. However, a significant effect of interaction between these two factors was found in only four proteins (4.9%): synapsin I ($F_{(1,16)}=4.871$, $p=0.042$), synaptophysin ($F_{(1,16)}=5.128$, $p=0.038$), septin 5 ($F_{(1,16)}=15.351$, $p=0.001$), and tyrosine 3-monooxygenase/ tryptophan 5-monooxygenase activation protein (YWHAE) ($F_{(1,16)}=5.359$, $p=0.034$). Among the 53 ApoE genotype dependent proteins, 32 (60.4%) were significantly lower and 21 (39.6%) were significantly higher in ApoE4 mice. Of the gender dependent proteins, 43 (97.7%) were significantly lower in female mice; only the expression of glutathione S-transferase Mu 1 (GSTM1) was increased.

Table 1. Quantitative proteomic analysis of the synaptosomal proteins involved in ApoE genotype- and gender-dependent responses

IPI number	Protein name	Gene symbol	2-way ANOVA			Ratio	
			ApoE genotype	Gender	Interaction	ApoE3/ApoE4	Male/female
Electron transport chain and oxidative phosphorylation							
IPI00120212	NADH dehydrogenase (ubiquinone) 1 alpha subcomplex, 9	*Ndufa9*	0.006**	0.072	0.487	1.83▲	1.43
IPI00308882	NADH dehydrogenase (ubiquinone) Fe-S protein 1	*Ndufs1*	0.026*	0.318	0.539	1.84▲	1.29
IPI00121309	NADH dehydrogenase (ubiquinone) Fe-S protein 3	*Ndufs3*	0.014*	0.728	0.454	1.77▲	1.07
IPI00130460	NADH dehydrogenase (ubiquinone) flavoprotein 1	*Ndufv1*	0.007**	0.008**	0.863	1.90▲	1.88▲
IPI00111885	Ubiquinol cytochrome c reductase core protein 1	*Uqcrc1*	0.004**	0.086	0.452	1.89▲	1.41
IPI00119138	Ubiquinol cytochrome c reductase core protein 2	*Uqcrc2*	0.047*	0.011*	0.587	1.39	1.56▲
IPI00133240	Ubiquinol-cytochrome c reductase, Rieske iron-sulfur polypeptide 1	*Uqcrfs1*	$<10^{4}$***	0.105	0.855	2.48▲	1.35
IPI00132728	Cytochrome c-1	*Cyc1*	0.181	0.035*	0.312	1.46	1.89▲
IPI00222419	Cytochrome c	*Cycs*	0.010**	0.062	0.934	1.48	1.31
IPI00114377	Cytochrome c oxidase, subunit VIIa 2	*Cox7a2*	0.044*	0.228	0.784	1.39	1.21
IPI00131176	Cytochrome c oxidase subunit 2	*Cox2*	0.035*	0.042*	0.711	1.57▲	1.54▲
IPI00230507	ATP synthase, H+ transporting, mitochondrial F0 complex, subunit d	*Atp5h*	0.938	0.039*	0.451	1.01	1.44
IPI00468481	ATP synthase, H+ transporting mitochondrial F1 complex, beta	*Atp5b*	0.042*	0.037*	0.978	1.29	1.3
IPI00313475	ATP synthase, H+ transporting, mitochondrial F1 complex, gamma polypeptide 1	*Atp5c1*	0.037*	0.137	0.285	1.42	1.27
IPI00118986	ATP synthase, H+ transporting, mitochondrial F1 complex, O subunit	*Atp5o*	0.058	0.010**	0.305	1.35	1.55▲
Glucose metabolism and tricarboxylic acid cycle							
IPI00228633	Glucose phosphate isomerase 1	*Gpi1*	0.055	0.035*	0.89	0.81	1.27
IPI00462072	Enolase 1	*Eno1*	0.76	0.036*	0.692	0.97	1.21
IPI00283611	Hexokinase 1	*Hk1*	0.132	0.003**	0.802	1.25	1.65▲
IPI00555060	Phosphoglycerate kinase 2	*Pgk2*	0.964	0.037*	0.716	0.99	1.63▲
IPI00119458	Aldolase C, fructose-bisphosphate	*Aldoc*	0.037*	0.716	0.517	0.79	0.96
IPI00113141	Citrate synthase	*Cs*	0.017*	0.036*	0.769	1.39	1.33
IPI00116074	Aconitase 2	*Aco2*	0.027*	0.015*	0.935	1.43	1.50▲
IPI00129928	Fumarate hydratase 1	*Fh1*	0.001***	0.028*	0.885	2.02▲	1.47
IPI00126635	Isocitrate dehydrogenase 3 (NAD+) beta	*Idh3b*	0.047*	0.054	0.807	1.60▲	1.57
IPI00323592	Malate dehydrogenase 2, NAD	*Mdh2*	0.004**	0.002**	0.714	1.42	1.49
Oxidative stress							
IPI00130589	Superoxide dismutase 1	*Sod1*	0.293	0.018*	0.917	1.1	1.27
IPI00109109	Superoxide dismutase 2	*Sod2*	0.001***	0.211	0.906	1.82▲	1.22
IPI00308885	Heat shock protein 1	*Shpd1*	0.353	0.005**	0.621	1.14	1.59▲
IPI00120045	Heat shock protein 1 (chaperonin 10)	*Shpe1*	0.138	0.010**	0.585	1.31	1.68▲
IPI00133903	Heat shock protein 9	*Shpa9*	0.035*	0.151	0.694	1.76▲	1.44
IPI00129517	Peroxiredoxin 5	*Prdx5*	0.019*	0.003**	0.14	1.4	1.57▲
IPI00230212	Glutathione S-transferase Mu 1	*Gstm1*	0.107	0.026*	0.399	0.68	0.57▲

Table 1. (*Cont.*)

IPI number	Protein name	Gene symbol	2-way ANOVA			Ratio	
			ApoE genotype	Gender	Interaction	ApoE3/ApoE4	Male/female
Lipid metabolism							
IPI00154054	Acetyl-Coenzyme A acetyltransferase 1	*Acat1*	0.1	0.004**	0.244	1.27	1.60▲
IPI00132653	3-oxoacid CoA transferase 1	*Oxct1*	0.08	0.014*	0.055	1.35	1.56▲
IPI00134809	Dihydrolipoamide S-succinyltransferase (E2 component of 2-oxo-glutarate complex)	*Dlst*	0.049*	0.112	0.59	1.73▲	1.54
IPI00153660	Dihydrolipoamide S-acetyltransferase (E2 component of pyruvate dehydrogenase complex)	*Dlat*	0.016*	0.207	0.353	1.49	1.21
IPI00337893	Pyruvate dehydrogenase E1 alpha 1	*Pdha1*	0.018*	0.019*	0.354	1.50▲	1.49
IPI00132042	Pyruvate dehydrogenase (lipoamide) beta	*Pdhb*	0.020*	0.020*	0.868	1.42	1.42
Microtubule stabilization and cytoskeletal organization							
IPI00115833	Microtubule-associated protein 6	*Mtap6*	$<10^{4}$***	0.721	0.34	0.57▲	1.04
IPI00117348	Tubulin, alpha 1B	*Tuba1b*	0.006**	0.102	0.56	0.78	1.14
IPI00224626	Septin 7	*Sept7*	0.006**	0.009**	0.918	0.62▲	1.56▲
IPI00416280	Septin 5	*Sept5*	0.166	0.57	0.001***	1.14	1.05
IPI00127942	Destrin	*Dstn*	0.863	0.007**	0.445	1.02	1.49
IPI00890117	Cofilin 1	*Cfl1*	0.928	0.003**	0.629	0.99	1.66▲
Amino acid metabolism							
IPI00117312	Glutamate oxaloacetate transaminase 2	*Got2*	0.021*	0.066	0.591	1.31	1.23
IPI00464317	Glutaminase	*Gls*	0.015*	0.186	0.116	1.91▲	1.37
IPI00626790	Glutamate-ammonia ligase (glutamine synthetase)	*Glul*	0.039*	0.194	0.506	0.8	1.14
IPI00114209	Glutamate dehydrogenase 1	*Glud1*	0.028*	0.035*	0.868	1.68▲	1.63▲
IPI00227445	4-aminobutyrate aminotransferase	*Abat*	0.027*	0.097	0.445	1.50▲	1.34
IPI00230289	Solute carrier family 1 (glial high affinity glutamate transporter), member 2	*Slc1a2*	0.015*	0.399	0.904	0.71	0.9
IPI00109275	Solute carrier family 25 (mitochondrial carrier, glutamate), member 22	*Slc25a22*	0.078	0.007**	0.905	1.25	1.44
Synaptogenesis and synaptic vesicle transmission							
IPI00131618	Syntaxin 1A	*Stx1a*	0.050*	0.34	0.831	0.75	1.14
IPI00113149	Syntaxin 1B	*Stx1b*	0.003**	0.931	0.848	0.69	0.99
IPI00136372	Synapsin I	*Syn1*	0.729	0.029*	0.042*	0.97	1.21
IPI00123505	Synaptophysin	*Syp*	0.189	0.377	0.038*	1.12	1.08
IPI00331579	Synaptogyrin 3	*Syngr3*	0.764	0.001***	0.406	1.05	2.00▲
IPI00116356	Adaptor protein complex AP-2, mu1	*Ap2m1*	0.037*	0.213	0.079	0.65▲	1.27
IPI00119113	ATPase, H+ transporting, lysosomal V1 subunit B2	*Atp6v1b2*	0.027*	0.477	0.161	0.77	1.08
IPI00331110	SH3-domain GRB2-like 2	*Sh3gl2*	0.149	0.016*	0.836	0.82	1.43
Other proteins							
IPI00556827	ATPase, Ca++ transporting, plasma membrane 1	*Atp2b1*	0.032*	0.26	0.28	0.37▲	1.6
IPI00311682	ATPase, Na+/K+ transporting, alpha 1 polypeptide	*Atp1a1*	0.042*	0.815	0.673	0.78	0.97
IPI00123704	ATPase, Na+/K+ transporting, beta 2 polypeptide	*Atp1b2*	0.004**	0.447	0.795	0.53▲	0.87
IPI00122048	ATPase, Na+/K+ transporting, alpha 3 polypeptide	*Atp1a3*	0.005**	0.306	0.657	0.77	1.09

IPI00126115	Sideroflexin 3	*Sfxn3*	0.004**	0.019*	0.674	1.78▲	1.56▲
IPI00128346	CDGSH iron sulfur domain 1	*Cisd1*	0.119	0.006**	0.808	1.31	1.68▲
IPI00131614	Synuclein, beta	*Sncb*	0.39	0.044*	0.506	0.86	1.46
IPI00313962	Ubiquitin carboxy-terminal hydrolase L1	*Uchl1*	0.011*	0.238	0.641	0.72	0.87
IPI00395193	Reticulon 1	*Rtn1*	0.018*	0.023*	0.985	0.68	1.45
IPI00229598	2′,3′-cyclic nucleotide 3′ phosphodiesterase	*Cnp*	0.010**	0.067	0.159	0.42▲	1.75
IPI00115546	Guanine nucleotide binding protein, alpha O	*Gnao1*	0.004**	0.585	0.712	0.72	1.06
IPI00323179	Guanosine diphosphate (GDP) dissociation inhibitor 1	*Gdi1*	0.094	0.033*	0.883	0.85	1.24
IPI00122547	Voltage-dependent anion-selective channel protein 2	*Vdac2*	0.042*	0.026*	0.964	1.56▲	1.65▲
IPI00124771	Solute carrier family 25 (mitochondrial carrier, phosphate carrier), member 3	*Slc25a3*	0.030*	0.091	0.906	1.65▲	1.46
IPI00121091	Proteolipid protein (myelin) 1	*Plp1*	0.003**	0.019*	0.593	0.40▲	1.70▲
IPI00115240	Myelin basic protein	*Mbp*	0.002**	0.036*	0.784	0.48▲	1.56▲
IPI00124830	CD47 antigen (Rh-related antigen, integrin-associated signal transducer)	*Cd47*	0.020*	0.066	0.365	0.64▲	0.71
IPI00112584	Calcium/calmodulin-dependent protein kinase II, delta	*Camk2d*	0.328	0.009**	0.754	0.91	1.34
IPI00118384	Tyrosine 3-monooxygenase/tryptophan 5-monooxygenase activation protein	*Ywhae*	0.295	0.606	0.034*	0.87	0.94
IPI00137730	Phosphatidylethanolamine binding protein 1	*Pebp1*	0.35	0.005**	0.757	0.86	1.67▲
IPI00122965	RAB3A, member RAS oncogene family	*Rab3a*	0.21	0.025*	0.783	1.25	1.54▲
IPI00321718	Prohibitin 2	*Phb2*	0.045*	0.028*	0.178	1.65▲	1.75▲

Each protein detected in all 20 mice samples of 13 mth was analysed by 2-way ANOVA (*$p<0.05$, **$p<0.01$, ***$p<0.001$). The ratios (ApoE3/ApoE4 or male/female) of 81 proteins were shown side by side [R=mean ApoE3/mean ApoE4 or R=mean male/mean female]. Proteins with >1.5-fold changes ($p<0.05$, 2-way ANOVA) are marked with triangle symbols.

Subsets of proteins with significantly altered expression were then grouped by genotype or gender, with a cut-off value of a 1.5-fold change ($p<0.01$) (Fig. 3, Table 1). The levels of seven proteins (NADH dehydrogenase 1 alpha sub-complex 9, NADH dehydrogenase flavoprotein 1, ubiquinol-cytochrome c reductase core protein 1, ubiquinol-cytochrome c reductase, Rieske iron-sulphur polypeptide 1, fumarate hydratase 1(FH1), SOD2 and sideroflexin 3) were significantly lower in ApoE4 mice compared with ApoE3 mice ($n=10$) (Fig. 3*a*). Interestingly, the expression of seven proteins (septin 7, syntaxin 1B, microtubule-associated protein 6, 2′,3′-cyclic nucleotide 3′ phosphodiesterase, myelin basic protein, proteolipid protein 1 and ATPase, Na^+/K^+ transporting, $\beta 2$ polypeptide), was significantly higher in ApoE4 mice ($n=10$) (Fig. 3*a*). Compared with males ($n=10$), the levels of all 11 proteins (NADH dehydrogenase flavoprotein 1, hexokinase 1, heat shock protein 1(HSPD1), heat shock protein 1 (chaperonin 10)(HSPE1), peroxiredoxin 5(PRDX5), acetyl-Coenzyme A acetyltransferase 1, septin 7, cofilin 1, CDGSH iron sulphur domain 1, phosphatidylethanolamine binding protein 1 and ATP synthase, H+ transporting, mitochondrial F1 complex, O subunit) were significantly lower in female mice ($n=10$) (Fig. 3*b*).

Oxidative phosphorylation and ATP synthesis were two of the most prominently affected pathways that were down-regulated in ApoE4 mice. Twelve proteins involved in complex I, III, IV and V of the electron transport chain (ETC) had significantly lower expression in ApoE4 mice (Supplementary Figure S2*a*, Table 1). Interestingly, cytochrome c levels were significantly lower in ApoE4 compared with ApoE3 mice ($p=0.01$, ratio=1.48). In addition, seven proteins related to the ETC complexes had significantly lower expression in female mice compared with males (Supplementary Figure S2*a*, Table 1).

Other pathways that play roles in the TCA cycle, glucose, lipid and amino acid metabolism were significantly down-regulated in ApoE4 and female mice, (Supplementary Figure S2*b*, Table 1). When the genotype effect was assessed, the levels of FH1 ($p=0.001$, ratio=2.02), pyruvate dehydrogenase E1 alpha 1 (PDHA1) ($p=0.018$, ratio=1.5) and glutamate dehydrogenase 1 (GLUD1) ($p=0.028$, ratio=1.68) were all significantly down-regulated in ApoE4 mice When the effect of gender was analysed, FH1 ($p=0.028$, ratio=1.47), PDHA1 ($p=0.019$, ratio=1.49) and GLUD1 ($p=0.035$, ratio=1.63) were significantly down-regulated in female mice.

Increased oxidative stress induced by ApoE4 and female risk factors

Reduced ETC efficiency and increased oxidative stress impairs neuronal function and exacerbates neurodegeneration. Among the proteins involved in oxidative stress pathway identified in our quantitative proteomice analysis, six of seven significant proteins (SOD1, SOD2, HSPD1, HSPE1, HSPA1 and PRDX5) exhibited reduced

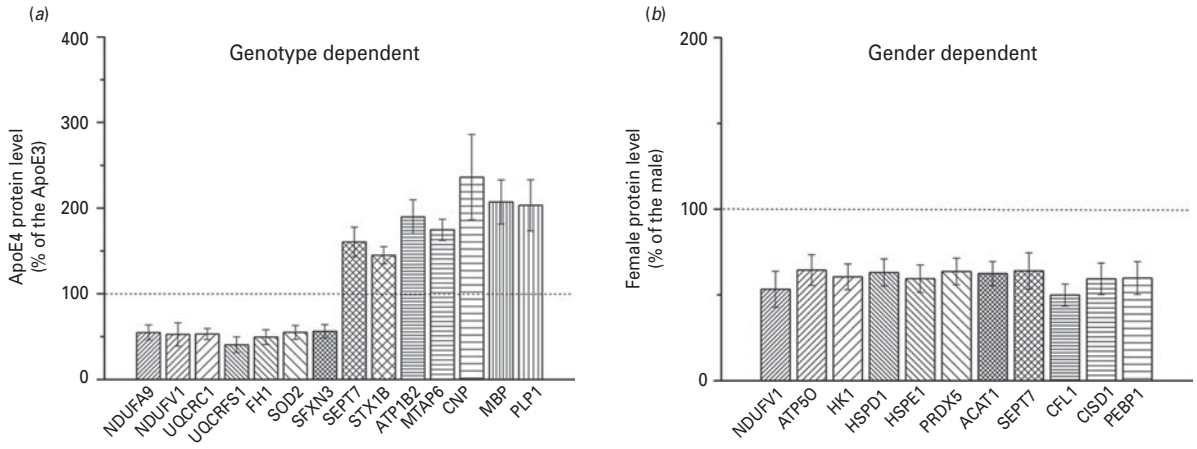

Fig. 3. The expression pattern of subsets of synaptosomal proteins with significant differences ($p<0.01$ and ratio >1.5). (*a*) Compared with ApoE3 mice, from SFXN3 to the left, the level of proteins were significantly lower in ApoE4 mice; from SEPT7 to the right, the level of proteins were significantly higher in ApoE4 mice. Every value of protein level in ApoE4 mice ($n=10$) was normalized to the mean of that protein's contents in ApoE3 mice ($n=10$). (*b*) Compared with males, the levels of proteins were significantly lower in female mice. Every value of protein level in female mice ($n=10$) was normalized to the mean of that protein's contents in male mice ($n=10$). The dashed line indicates the relative protein level of control (ApoE3 or male group). Values are presented as mean±S.E.M.

expression in ApoE4 or female mice, except for GSTM1 (Table 1). In particular, SOD2 ($p=0.001$, ratio=1.82) and PRDX5 ($p=0.003$, ratio=1.57) were significantly lower in ApoE4 and female mice (both $n=10$). Interestingly, when gender-dependent proteome alterations were assessed, only GSTM1 was significantly up-regulated, and was ~1.75-fold higher in female than male mice ($p=0.026$, ratio=0.57).

COXIV and SOD2 play an important role in maintaining the redox balance. Therefore, Western blotting validated their expression levels. The levels of COXIV ($p=0.018$, ratio=1.51) and SOD2 ($p=0.002$, ratio=1.39) were significantly lower in ApoE4 mice compared with ApoE3 mice ($n=10$) (Fig. 4*a*, *c*). Similarly, the levels of both proteins (COXIV: $p=0.023$, ratio=1.48; SOD2: $p=0.002$, ratio=1.40) were significantly lower in female mice compared with male mice ($n=10$) (Fig. 4*b*, *d*).

The GSH/GSSG ratio and MDA levels are considered to be indicators of oxidative stress. Our results demonstrate that GSSG levels were increased significantly in ApoE4 ($n=10$) compared with ApoE3 animals ($n=10$) ($p=0.005$, ratio=0.61) (Fig. 5*b*). Similarly when ApoE4 females ($n=10$) and ApoE4 males ($n=10$) were compared ($p=0.003$, ratio=0.58), there was also an increase (Fig. 5*f*), In contrast, there was no significant difference in GSH levels in the mouse cortex between genotypes (Fig. 5*a*) or genders (Fig. 5*e*). Furthermore, ApoE4 mice ($n=10$) had a lower GSH/GSSG ratio than ApoE3 mice ($n=10$) ($p=0.025$, ratio=1.50) (Fig. 5*c*) and a similar result was observed in female mice compared with male mice ($n=10$) ($p=0.027$, ratio=1.49) (Fig. 5*g*). Consistent with above data, MDA levels were also higher in ApoE4 ($n=10$) ($p<0.001$, ratio=0.78) (Fig. 5*d*) and female mice ($n=10$) ($p=0.012$, ratio=0.86) (Fig. 5*h*).

Synaptic termini were more susceptible to damage than non-synaptic mitochondria in the soma

To assess if the ApoE genotype or gender caused detrimental effects in synaptic termini and non-synaptic mitochondrial fractions, the ratio of protein abundance between ApoE genotypes or genders was used as an indicator. We identified 503 proteins after protein rollup in the non-synaptic mitochondria isolated from 20 mice cortices. Of these, 44 mitochondrial-related proteins were detected in both non-synaptic mitochondrial and synaptosomal fractions from all 20 samples (Table 2). In the non-synaptic mitochondria, there were no significant proteomic differences in these 44 mitochondrial-related proteins between genotypes, and only 10 proteins were decreased significantly in female, with a mean reduction of ~1.7-fold (Fig. 6*a*, *c*, Table 2). In contrast, 31 of the 44 mitochondrial-related proteins, were decreased significantly, with a mean of ~1.6-fold, in the synaptosomes in ApoE4 mice. Similarly, 26 proteins were decreased significantly, with a mean of ~1.5-fold in female (Fig. 6*b*, *d*, Table 2).

Reduced oestrogen levels in female ApoE4 mice cortices and significantly enhanced neuroprotective effects of oestrogen in ApoE3-C6 cells

To investigate the possible mechanism underlying the gender-related differences in the oxidative stress response to ApoE genotype, the levels of local oestradiol in the cortex of ApoE transgenic mice were measured. The results demonstrated that the oestrogen levels in ApoE4 mice showed a downward trend compared with ApoE3 mice in the cortex, but not in serum (Fig. 7*a*, $p=0.06$). Importantly, ApoE4 female mice had significantly

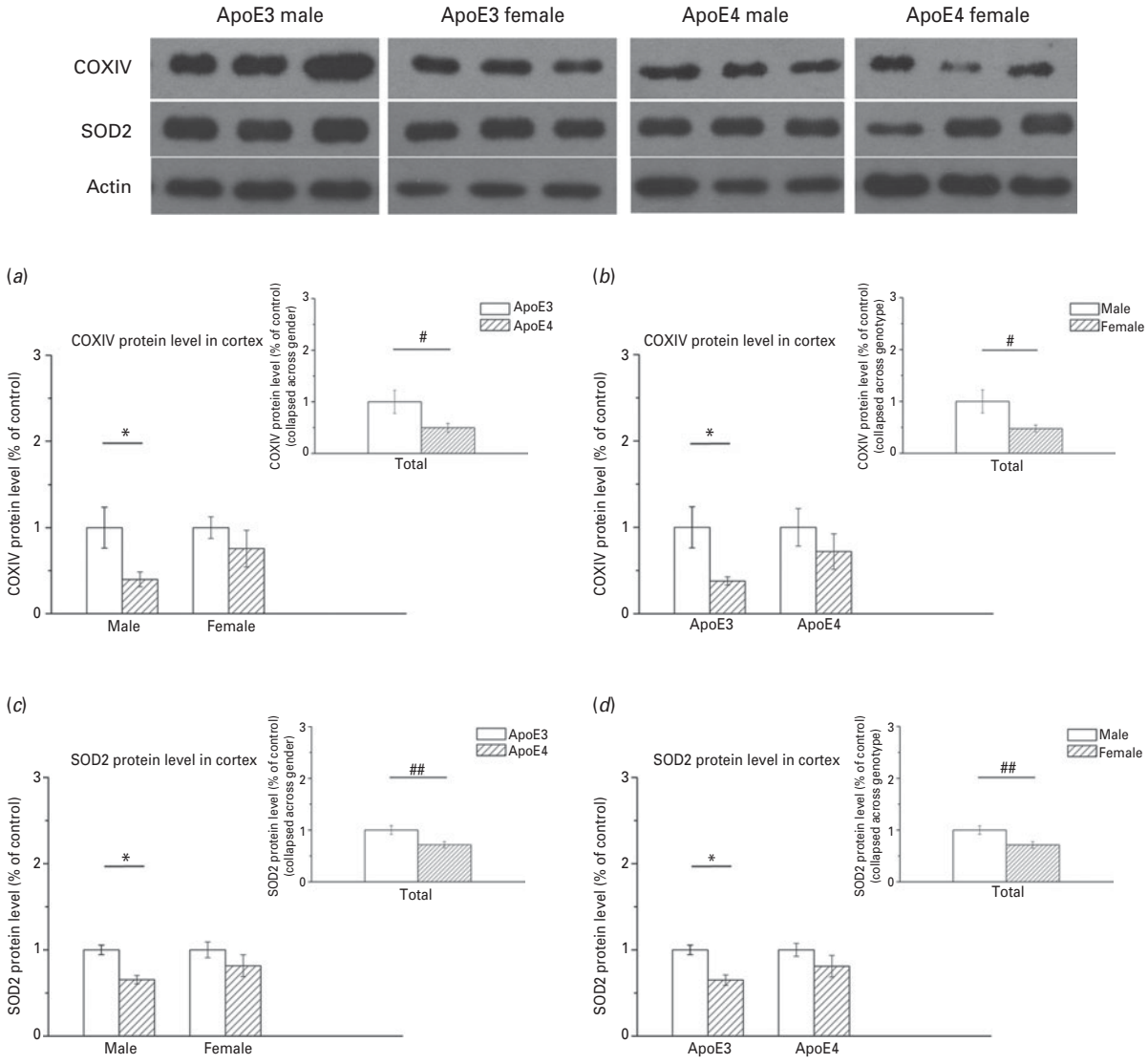

Fig. 4. Expression of COXIV and SOD2 in mice cortices (*a, c*).The protein levels of COXIV and SOD2 were significantly lower in ApoE4 compared with ApoE3 mice. (*b, d*) The levels of COXIV and SOD2 were also significantly lower in female compared with male mice. The insets show the protein level assessed by genotype or gender because there was no interaction between the genotype and gender factors. (Values are presented as mean±S.E.M; $n=5$ per genotype or gender; *t* test: $^{*}p<0.05$; 2-way ANOVA: $^{\#}p<0.05$, $^{\#\#}p<0.01$).

reduced oestrogen levels compared with ApoE3 female mice (Fig. 7*b*, $p<0.05$), whereas there was no difference between two ApoE genotypes in the cortices of males. Surprisingly, the expression levels of *aromatase*, which is a key enzyme during oestrogen synthesis, in the cortices was significantly up-regulated in ApoE4 mice compared with ApoE3 mice, particularly in ApoE4 female mice (Fig. 7*c*, $p<0.05$).

We next further evaluated whether different ApoE genotypes might affect the protective effects of oestrogen. Oxidative stress was induced in the human ApoE-stable transfected C6 cells by treating with 500 μM H_2O_2 for 24 h. An MTT assay then revealed that H_2O_2 exposure was toxic to both ApoE3 and ApoE4 C6 cells. However, ApoE3-C6, but not ApoE4-C6 cells exhibited significantly decreased H_2O_2 toxicity after treatment with oestrogen. As a rapid compensatory effect, the mRNA levels of *COXIV* and *SOD2* were increased (Fig. 8). Surprisingly, oestrogen significantly down-regulated the expression of *COXIV* and *SOD2* mRNA in ApoE3-C6 compared with ApoE4-C6 cells in response to oxidative stress damage (Fig. 8, $p<0.05$).

Discussion

This present study demonstrates that the expression patterns of the synaptosomal proteome in ApoE transgenic mice were significantly affected not only by the ApoE genotype, but also by gender. Furthermore, the greater detrimental effects of the ApoE4 genotype

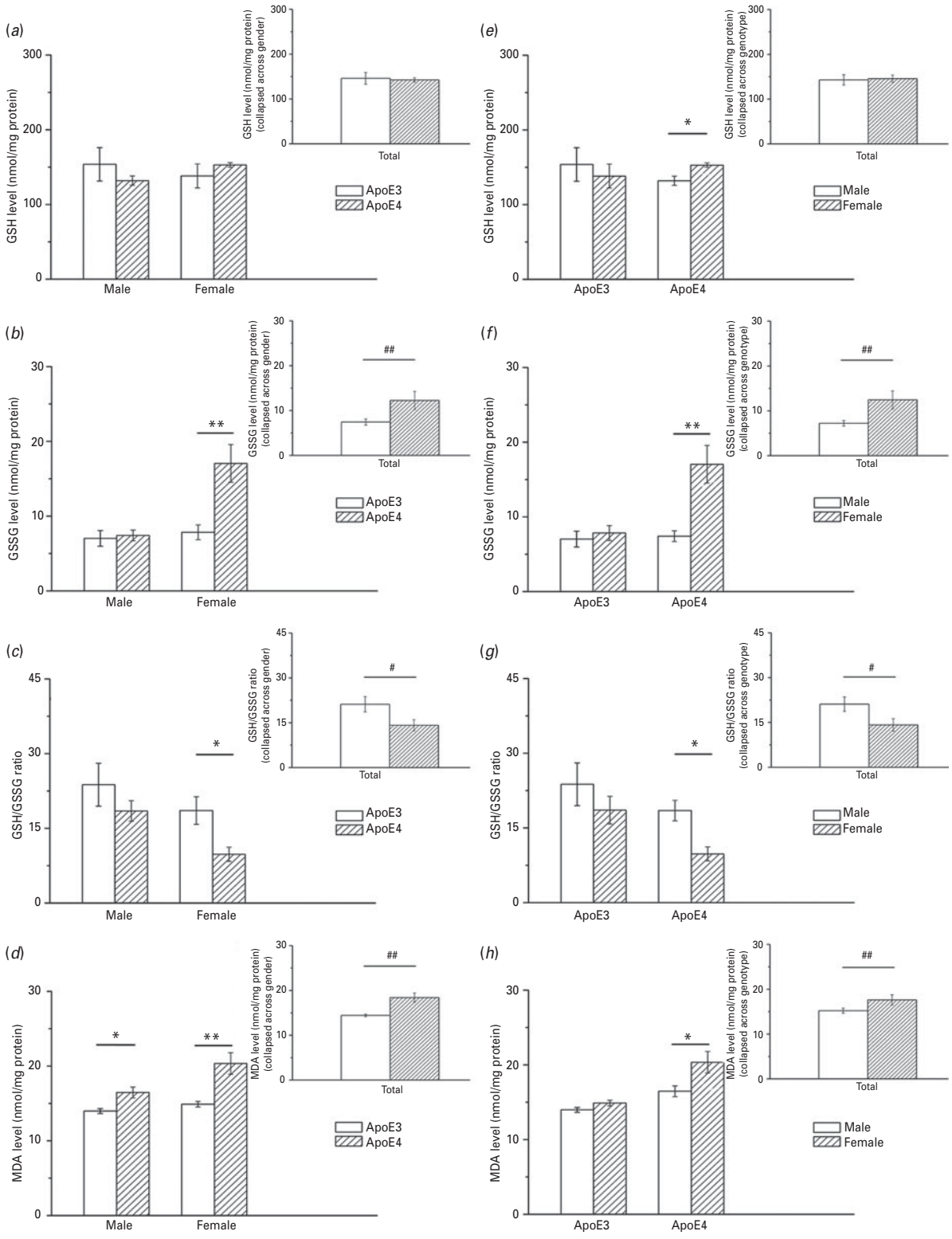

Fig. 5. Increased oxidative stress in the cortices of ApoE4 and female mice. (*a–h*) The insets show the levels of oxidative stress across genotype or gender because there was no interaction between the genotype and gender factors. (Values are presented as mean±S.E.M; $n=5$ per genotype or gender; *t* test: $^{*}p<0.05$, $^{**}p<0.01$; 2-way ANOVA: $^{\#}p<0.05$, $^{\#\#}p<0.01$).

in female, compared with male mice are consistent with the epidemiological evidence reporting of ApoE4 and gender as risk factors for the development of AD in humans. These early detrimental effects might accumulate predominantly in the synaptic terminals, but not in the neural soma. Oestrogen levels in females, which were affected by the ApoE4 genotype, might alter the synaptosomal proteome and synaptic

Table 2. The proteomic response of non-synaptic mitochondria far away from synaptic terminals to the ApoE3/4 genotype or gender factor

IPI number	Protein name	Gene symbol	Ratio (non-synaptic mitochondria)		Ratio (synaptosome)	
			ApoE3/ApoE4	Male/female	ApoE3/ApoE4	Male/female
Electron transport chain and oxidative phosphorylation						
IPI00120212	NADH dehydrogenase (ubiquinone) 1 alpha sub-complex, 9	*Ndufa9*	1.07	1.25	1.83**	1.43
IPI00308882	NADH dehydrogenase (ubiquinone) Fe-S protein 1	*Ndufs1*	0.88	1.2	1.84*	1.29
IPI00121309	NADH dehydrogenase (ubiquinone) Fe-S protein 3	*Ndufs3*	1.09	1.27	1.77*	1.07
IPI00130460	NADH dehydrogenase (ubiquinone) flavoprotein 1	*Ndufv1*	0.88	1.39	1.9**	1.88**
IPI00111885	Ubiquinol cytochrome c reductase core protein 1	*Uqcrc1*	1.12	1.41*	1.89**	1.41
IPI00119138	Ubiquinol cytochrome c reductase core protein 2	*Uqcrc2*	1.19	1	1.39*	1.56*
IPI00133240	Ubiquinol-cytochrome c reductase, Rieske iron-sulphur polypeptide 1	*Uqcrfs1*	1.25	1.26	2.48***	1.35
IPI00132728	Cytochrome c-1	*Cyc1*	1.07	1.6*	1.46	1.89*
IPI00222419	Cytochrome c	*Cycs*	1.11	1.27	1.48**	1.31
IPI00114377	Cytochrome c oxidase, subunit VIIa 2	*Cox7a2*	0.99	1.58*	1.39*	1.21
IPI00230507	ATP synthase, H+ transporting, mitochondrial F0 complex, subunit d	*Atp5h*	0.99	1.37	1.01	1.44*
IPI00468481	ATP synthase, H+ transporting mitochondrial F1 complex, beta subunit	*Atp5b*	0.98	1.35	1.29*	1.3*
IPI00313475	ATP synthase, H+ transporting, mitochondrial F1 complex, gamma polypeptide 1	*Atp5c1*	1.03	1.54	1.42*	1.27
IPI00118986	ATP synthase, H+ transporting, mitochondrial F1 complex, O subunit	*Atp5o*	0.95	0.6	1.35	1.55**
Glucose metabolism and tricarboxylic acid cycle						
IPI00462072	Enolase 1	*Eno1*	1.32	1.04	0.97	1.21*
IPI00283611	Hexokinase 1	*Hk1*	0.97	1.86*	1.25	1.65*
IPI00113141	Citrate synthase	*Cs*	0.89	2.08*	1.39*	1.33*
IPI00116074	Aconitase 2	*Aco2*	1.12	1.34	1.43*	1.5*
IPI00129928	Fumarate hydratase 1	*Fh1*	1.2	1.69	2.02***	1.47*
IPI00126635	Isocitrate dehydrogenase 3 (NAD+) beta	*Idh3b*	0.97	1.18	1.6*	1.57
IPI00323592	Malate dehydrogenase 2, NAD	*Mdh2*	1	1.66*	1.42**	1.49**
Oxidative stress						
IPI00130589	Superoxide dismutase 1	*Sod1*	1.23	1.73*	1.1	1.27*
IPI00109109	Superoxide dismutase 2	*Sod2*	1.3	1.4	1.82***	1.22
IPI00308885	Heat shock protein 1	*Hspd1*	0.83	1.69	1.14	1.59**
IPI00120045	Heat shock protein 1 (chaperonin 10)	*Hspe1*	0.95	1.36	1.31	1.68**
IPI00133903	Heat shock protein 9	*Hspa9*	1.24	1.3	1.76*	1.44
IPI00129517	Peroxiredoxin 5	*Prdx5*	0.86	1.39	1.4*	1.57**
Lipid metabolism						
IPI00154054	Acetyl-Coenzyme A acetyltransferase 1	*Acat1*	1.1	1.38	1.27	1.6**
IPI00132653	3-oxoacid CoA transferase 1	*Oxct1*	1.05	1.32	1.35	1.56*
IPI00134809	Dihydrolipoamide S-succinyltransferase (E2 component of 2-oxo-glutarate complex)	*Dlst*	1.28	1.42	1.73*	1.54
IPI00153660	Dihydrolipoamide S-acetyltransferase (E2 component of pyruvate dehydrogenase complex)	*Dlat*	1.14	1.19	1.49*	1.21
IPI00337893	Pyruvate dehydrogenase E1 alpha 1	*Pdha1*	1.22	1.59*	1.5*	1.49*
IPI00132042	Pyruvate dehydrogenase (lipoamide)	*Pdhb*	0.91	1.82*	1.42*	1.42*
Amino acid metabolism						
IPI00117312	glutamate oxaloacetate transaminase 2	*Got2*	1.12	1.42	1.31*	1.23
IPI00464317	glutaminase	*Gls*	1.04	1.7	1.91*	1.37

Table 2. (*Cont.*)

IPI number	Protein name	Gene symbol	Ratio (non-synaptic mitochondria)		Ratio (synaptosome)	
			ApoE3/ApoE4	Male/female	ApoE3/ApoE4	Male/female
IPI00114209	glutamate dehydrogenase 1	*Glud1*	1.11	1.14	1.68*	1.63*
IPI00227445	4-aminobutyrate aminotransferase	*Abat*	0.95	1.4	1.5*	1.34
IPI00109275	solute carrier family 25 (mitochondrial carrier, glutamate), member 22	*Slc25a22*	1.26	1.28	1.25	1.44**
Other proteins						
IPI00122048	ATPase, Na+/K+ transporting, alpha 3 polypeptide	*Atp1a3*	0.92	2.13*	0.77**	1.09
IPI00126115	sideroflexin 3	*Sfxn3*	0.87	1.5	1.78**	1.56*
IPI00128346	CDGSH iron sulfur domain 1	*Cisd1*	0.91	1.28	1.31	1.68**
IPI00122547	Voltage-dependent anion-selective channel protein 2	*Vdac2*	1.08	1.28	1.56*	1.65*
IPI00124771	Solute carrier family 25 (mitochondrial carrier, phosphate carrier), member 3	*Slc25a3*	1.09	2.32	1.65*	1.46
IPI00321718	prohibitin 2	*Phb2*	0.94	0.88	1.65*	1.75*

Forty-four mitochondrial-related proteins detected in both non-synaptic mitochondrial and synaptosomal fractions of all twenty mice were analysed using 2-way ANOVA (*$p<0.05$, **$p<0.01$, ***$p<0.001$). The protein ratios (ApoE3/ApoE4 or male/female) are shown side by side [R=mean ApoE3/mean ApoE4 or R=mean male/mean female]. There was no interaction between genotype and gender.

oxidative stress leading to the neuronal injury as AD progresses.

Previous studies suggested that astrocyte-secreted, human ApoE4-relpacement transgenic mice were useful models of AD (Sun et al., 1998). ApoE, which is mainly secreted by glial cells, plays a key role in the central nervous system (Holtzman et al., 2012). The loss of neurons and synapses in the cerebral cortex are classical pathological features in AD. Synaptosomes (a research model for neuronal and synaptic function) contain the complete synaptic molecular structure and are functional, with the ability to uptake, store, and release neurotransmitters (Whittaker, 1993; Ashton and Ushkaryov, 2005). Synaptosomal proteomics has been used to scrutinize global changes in synaptic proteins and aberrant synapse physiology, which is thought to be the basis of various brain disorders (Li and Jimenez, 2008; Bayes and Grant, 2009).

Our results of synaptosomal proteomic profiling revealed that the proteins that were significantly regulated by the ApoE genotype were mainly involved in metabolism and mitochondrial function. Perturbations in the physiological function of mitochondria and increased oxidative stress inevitably disturb neuronal function, which is intimately associated with the development and progression of AD (Moreira et al., 2005; Lin and Beal, 2006). Impairment in the ETC, particularly in COX, was recently linked to the onset of sporadic AD. This is consistent with our previous findings, where the brain protein levels of cytochrome c oxidase subunits were also lower in AD, as assessed by Western blotting (Kish et al., 1999) and microarray analyses (Xu et al., 2006). SOD2 is a key enzyme that is responsible for the mitochondrial detoxification of ROS. A previous report demonstrated that over-expression of SOD2 reduced hippocampal superoxide and prevented memory deficits in an AD mouse model (Massaad et al., 2009). Consistent with those findings, our results demonstrated that SOD2 was significantly down-regulated in ApoE4 mice.

Consistent with many observations in AD patients, our results also showed that ApoE4-associated neuropathology might occur via the disruption of mitochondrially regulated lipid, amino acid, energy and glucose metabolism. For example, dihydrolipoamide S-succinyltransferase, pyruvate dehydrogenase E1 alpha 1, glutaminase, glutamate dehydrogenase 1, 4-aminobutyrate aminotransferase, fumarate hydratase 1 and isocitrate dehydrogenase 3 (NAD+) beta were all decreased significantly by >1.5-fold in ApoE4 compared with ApoE3 mice. The hypothesis that increased oxidative stress caused mitochondrial dysfunction via unknown mechanisms was further supported by the presence of markers of lipid peroxidation and the glutathione system in thirteen-month-old ApoE4 transgenic mice. Mahley et al. (2009) and Chen et al. (2011b) have both reported that the structural differences between ApoE4 and ApoE3, contribute to the regulation of their diverse biological functions.

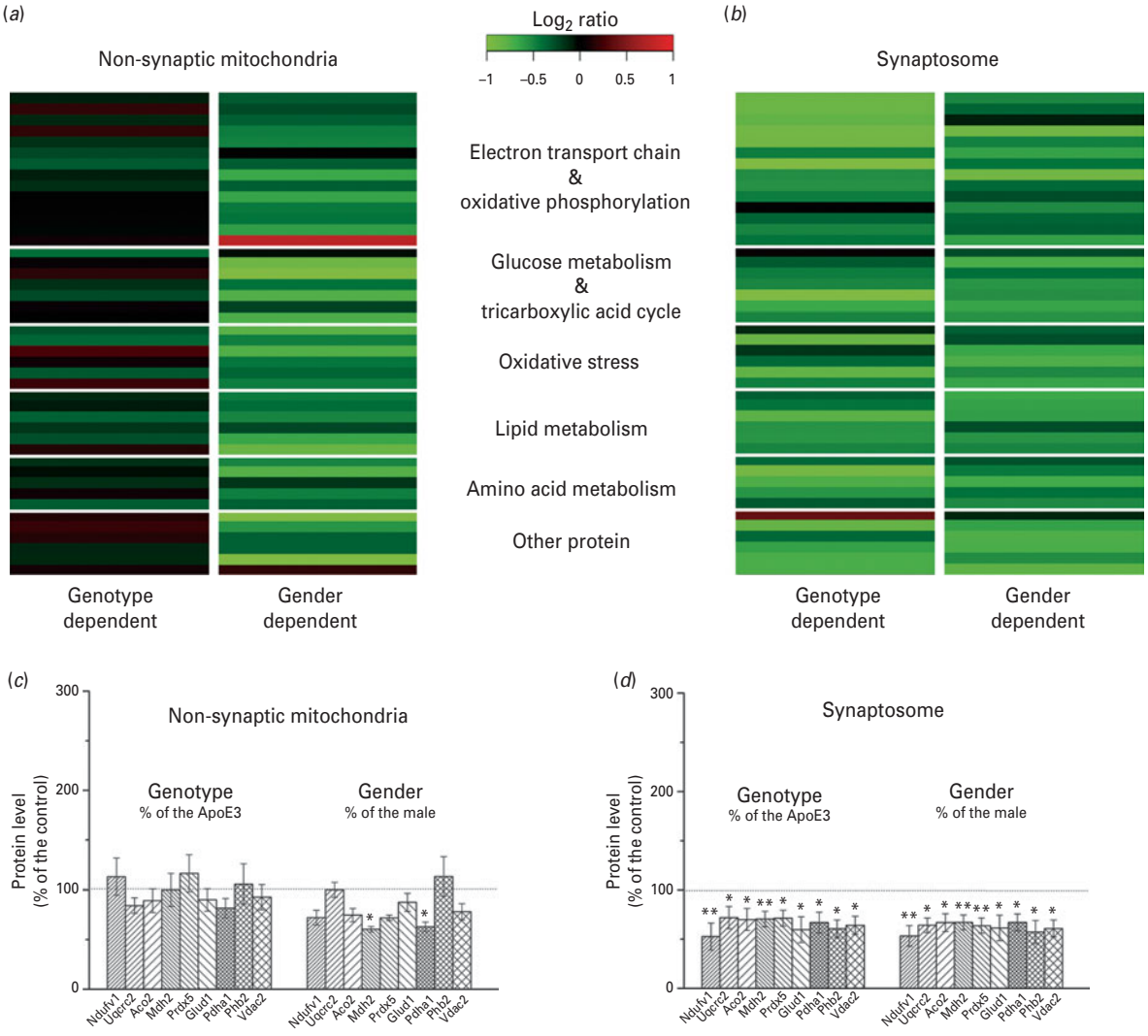

Fig. 6. The proteome profiling of non-synaptic mitochondria far away from synaptic terminals. (*a*) The genotype- and gender-dependent effects on mitochondrial-related protein expression are shown in non-synaptic mitochondria (*b*) Similarly, the genotype- and gender-dependent effects on mitochondrial-related protein expression are shown in synaptosomes. The $\log_2$ ratios (ApoE4/ApoE3 or female/male) of 44 mitochondrial-related proteins identified in both non-synaptic mitochondrial and synaptosomal fractions from all twenty samples are shown side by side [M=$\log_2$ (mean $_{ApoE4}$/mean $_{ApoE3}$) or M=$\log_2$ (mean $_{female}$/mean $_{male}$)]. Red and green colours represent increased or decreased fold changes, respectively. (*c, d*) Representative protein expression patterns affected by the genotype or gender factor in the non-synaptic mitochondria and synaptosomes are shown respectively. The protein levels in ApoE4 or female mice were normalized to the mean of protein content in the corresponding control group. The dashed line indicates the relative protein level of controls (ApoE3 or male group). (Values are presented as mean±S.E.M.; n=10 per genotype or gender; 2-way ANOVA, *p<0.05, **p<0.01, ***p<0.001).

Gender differences in cognitive function are well documented, in both rodents (Gresack and Frick, 2003) and humans (Astur et al., 2004; Postma et al., 2004). Recent studies have used stereological and correlative light and electron microscopy to reveal that males have a significantly higher synaptic density than females in all cortical layers of the temporal neocortex, (Alonso-Nanclares et al., 2008). Similarly, we found that nearly all proteins from the synaptosomes were down-regulated in the female mouse proteome. Gender differences in oxidative stress were also clearly observed in our experiments (Figs. 2–5). When the female gender and ApoE4 risk factors were combined, these effects were even more profound. Our proteomic results demonstrate that the relative changes in proteins induced specifically by the female risk factor had a similar trend to those induced by ApoE4 factor, particularly for NADH dehydrogenase (ubiquinone) flavoprotein 1, cytochrome c oxidase subunit 2, glutamate dehydrogenase 1, VDAC2 and prohibitin 2 (p<0.05, ratio>1.5). Surprisingly, however, of the 44 proteins that were significantly altered by the female-specific risk factor, only GSTM1 was up-regulated (p<0.05, ratio>1.75). Similar to its the role in maintaining the redox balance, GSTM1 might also play an important

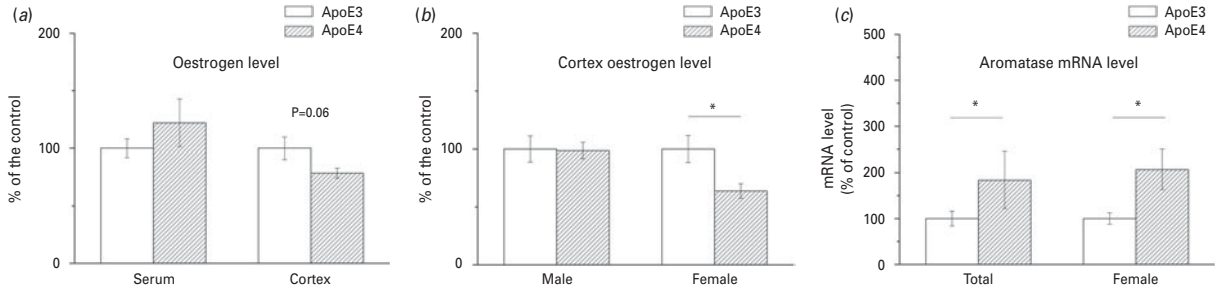

Fig. 7. Oestrogen levels in the cortices of 13-month-old ApoE transgenic mice. (*a*) ApoE genotype affects oestrogen levels more in the cortex than serum. (*b*) Oestrogen levels in the cortex were significantly decreased in ApoE4 compared with ApoE3 female mice. (*c*) There was a significant compensatory increase in *aromatase* mRNA levels in the cortex of ApoE4 mice, particularly in females. (Values are presented as mean±S.E.M; *t*-test: *$p<0.05$; $n=9$–11 per group).

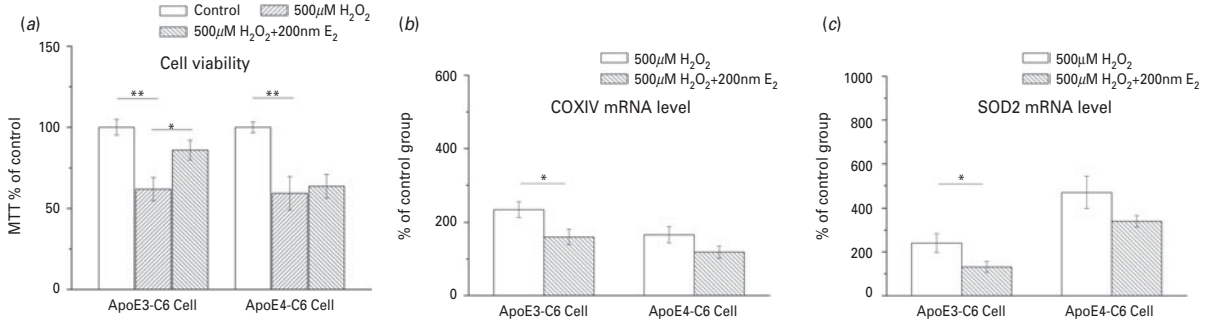

Fig. 8. Protective effects of 17β-dial (E_2) against oxidative stress injury induced by H_2O_2 in different ApoE stably transfected C6 cells. (*a*) H_2O_2-induced toxicity was decreased significantly in ApoE3-C6, but not ApoE4-C6, cells by treatment oestrogen compared to ApoE4-C6 cell. (*b, c*) *COXIV* and *SOD2* mRNA levels were increased significantly after oxidative stress injury compared with control. After treatment with E_2 (200 nM), *COXIV* and *SOD2* mRNA levels were significantly decreased only in ApoE3-C6 cells. Values are presented as mean±S.E.M; *t*-test: *$p<0.05$, $n=5$.

role in SOD2 null mice (Hinerfeld et al., 2004). Consistent with our findings, a previous study reported that female mice were more susceptible to ApoE4-induced cognitive impairment than male mice (Raber et al., 2000). These findings might provide a reasonable explanation as to why elderly females, particularly those carrying the ApoE ε4 allele, have a higher risk of developing AD than males (Payami et al., 1996).

Generally, sex hormones play a dominant role in modulating gender-based physiological differences. Previous studies reported that the decrease in oestrogen in females after menopause is a likely risk factor for AD (Wickelgren, 1997; Yue et al., 2005), and that oestrogen might also play an important role in oxidative stress. Interestingly, our data demonstrated that oestrogen levels could be modulated by the ApoE genotype in the cortex, but not in the serum. ApoE4 could affect oestrogen levels by regulating the hormone metabolism in brain. The compensatory increase in *aromatase* mRNA, which was affected by the ApoE4 genotype might be a possible explanation for the reduced oestrogen levels. However, the activity of aromatase might be another important factor that affects the oestrogen expression. Our proteomic data also showed that the expression of hydroxysteroid (17-beta) dehydrogenase 10, which is essential for maintaining the appropriate levels of sex hormones (Yang et al., 2005), was down-regulated by both ApoE4 genotype and female gender. A substantial and growing body of literature suggests that oestrogens exert their potent neuroprotective effects via a direct or indirect mitochondrial mechanism (Singh et al., 2006; Brinton, 2008b). Recently, a proteomic study suggested that 17β-oestradiol(E_2) regulated mitochondrial function, and specifically increased key elements in the TCA cycle, pyruvate metabolism, oxidative phosphorylation, respiratory efficiency and ATP generation, while reducing free radical leakage and oxidative damage (Nilsen et al., 2007). In contrast, a lack of protection from oestrogen increased mitochondrial ROS production (Numakawa et al., 2011) and the dysregulation of Ca^{2+} homeostasis (Brinton, 2008a). This might cause synaptic dysfunction, leading to neuronal injury in the early stages of AD. In the current study, the protective effects of oestrogen were only found in ApoE3 cells. Consistent with this, the ApoE4 genotype reduced the neuroprotective effect of E_2 in an animal model (Brown et al., 2008) Although its mechanism of action remains unclear, ApoE4 was reported to have isoform specific effects on signal transduction pathways including ERK and JNK (Ohkubo et al., 2001; Korwek et al., 2009). In addition, oestrogen-mediated signalling involved activation

of the ERK and JNK pathways (Cui et al., 2013). Therefore, it is possible that oestrogen signalling is defective in the ApoE4 genotype. Furthermore, the results of our study might explain why oestrogen replacement therapy was associated with reduced cognitive decline among ApoE4-negative females (Yaffe et al., 2000).

Our proteomic analyses indicated that synaptic terminals were more susceptible to oxidative stress damage that was affected by the ApoE genotype and gender factors. In synaptic mitochondria, 72.7 and 59% proteins were significantly affected by the ApoE genotype and gender factors, respectively (Table 2, Fig. 6). However, only 22.7% proteins were significantly affected by gender, and none were significantly regulated by ApoE genotype in non-synaptic mitochondria (Table 2, Fig. 6). The expression levels of voltage-dependent anion-selective channel protein 2(VDAC2) and prohibitin 2, which are located in the outer and inner mitochondrial membranes respectively, were comparable in the non-synaptic mitochondria from either genotype or gender. In contrast, the levels of these two proteins were significantly down-regulated in ApoE4 and female mice in the synaptosomes. The differential expression of PRDX5 (an antioxidant enzyme), which was affected by ApoE4 genotype and female gender, also has a similar synaptic regional specificity. These findings are interesting and the down-regulation of these evolutionarily conserved and multifunctional proteins could induce changes in mitochondrial function, leading to excessive ROS production. Recently, many studies have supported the notion that prohibitins participate in mitochondrial dynamics and stabilize the oxidative phosphorylation system (Artal-Sanz and Tavernarakis, 2009). The deletion of VDAC2 enhanced the activation of mitochondrial apoptosis (Cheng et al., 2003). PRDX5 confers protection against oxidative stress and promotes longevity in *Drosophila melanogaster* (Radyuk et al., 2009). Consistent with our findings, recent studies also reported the regional specificity of the mitochondria in neurons, and also proposed that synaptic mitochondria are long-lived, but more vulnerable to cumulative damage than non-synaptic mitochondria. In addition, synaptic mitochondria were more susceptible to Aβ-induced damage than mitochondria located in other regions in an AD mouse model (Du et al., 2010). Other reports also demonstrated that synaptic mitochondria might initiate neuronal death in response to insults, increasing the synaptic levels of intracellular Ca^{2+} (Brown et al., 2006). Therefore, significant evidence suggests that defects in synaptic mitochondria can likely lead to synaptic dysfunction and the loss of the synapses, which lead to alterations in cognitive function during AD.

Our findings revealed that the abnormal metabolism in the synapse and increased oxidative stress might represent a functional convergence of the ApoE4 and gender risk factors. Furthermore, the synaptic terminal is more vulnerable to cumulative oxidative stress damage induced by the ApoE4 genotype or female gender. The decreased oestrogen levels in the cortex observed with the ApoE4 genotype might limit the neuroprotective effects of oestrogen against oxidative stress, which leads to synaptic dysfunction and further neuronal injury.

Supplementary material

For supplementary material accompanying this paper, visit http://dx.doi.org/10.1017/S1461145714000601

Acknowledgments

We thank Professor Qiang Liu, Dr Hui Fang, Dr Yajing Liu and Dr Lifeng Zhang for technical support and constructive comments. This study was supported by the Natural Science Foundation of China (30870822), National Basic Research Program of China (2012CB947602) and the Ministry of Science and Technology of China (2011CB504100).

Statement of Interest

None.

References

Alonso-Nanclares L, Gonzalez-Soriano J, Rodriguez JR, DeFelipe J (2008) Gender differences in human cortical synaptic density. Proc Natl Acad Sci USA 105:14615–14619.

Artal-Sanz M, Tavernarakis N (2009) Prohibitin and mitochondrial biology. Trends Endocrinol Metab 20:394–401.

Ashton AC, Ushkaryov YA (2005) Properties of synaptic vesicle pools in mature central nerve terminals. J Biol Chem 280:37278–37288.

Astur RS, Tropp J, Sava S, Constable RT, Markus EJ (2004) Sex differences and correlations in a virtual Morris water task, a virtual radial arm maze, and mental rotation. Behav Brain Res 151:103–115.

Avramopoulos D (2009) Genetics of Alzheimer's disease: recent advances. Genome Med 1:34.

Bayes A, Grant SG (2009) Neuroproteomics: understanding the molecular organization and complexity of the brain. Nat Rev Neurosci 10:635–646.

Brinton RD (2008a) Oestrogen regulation of glucose metabolism and mitochondrial function: therapeutic implications for prevention of Alzheimer's disease. Adv Drug Deliv Rev 60:1504–1511.

Brinton RD (2008b) The healthy cell bias of oestrogen action: mitochondrial bioenergetics and neurological implications. Trends Neurosci 31:529–537.

Brown CM, Choi E, Xu Q, Vitek MP, Colton CA (2008) The APOE4 genotype alters the response of microglia and macrophages to 17beta-oestradiol. Neurobiol Aging 29:1783–1794.

Brown MR, Sullivan PG, Geddes JW (2006) Synaptic mitochondria are more susceptible to Ca2+overload than nonsynaptic mitochondria. J Biol Chem 281:11658–11668.

Chen HK, Ji ZS, Dodson SE, Miranda RD, Rosenblum CI, Reynolds IJ, Freedman SB, Weisgraber KH, Huang Y,

Mahley RW (2011a) Apolipoprotein E4 domain interaction mediates detrimental effects on mitochondria and is a potential therapeutic target for Alzheimer disease. J Biol Chem 286:5215–5221.

Chen J, Li Q, Wang J (2011b) Topology of human apolipoprotein E3 uniquely regulates its diverse biological functions. Proc Natl Acad Sci USA 108:14813–14818.

Cheng EH, Sheiko TV, Fisher JK, Craigen WJ, Korsmeyer SJ (2003) VDAC2 inhibits BAK activation and mitochondrial apoptosis. Science 301:513–517.

Cui J, Shen Y, Li R (2013) Oestrogen synthesis and signaling pathways during aging: from periphery to brain. Trends Mol Med 19:197–209.

Damoiseaux JS, Seeley WW, Zhou J, Shirer WR, Coppola G, Karydas A, Rosen HJ, Miller BL, Kramer JH, Greicius MD (2012) Gender modulates the APOE epsilon4 effect in healthy older adults: convergent evidence from functional brain connectivity and spinal fluid tau levels. J Neurosci 32:8254–8262.

De Jager PL et al. (2012) A genome-wide scan for common variants affecting the rate of age-related cognitive decline. Neurobiol Aging 33:1017, e1011–1015.

Du H, Guo L, Yan S, Sosunov AA, McKhann GM, Yan SS (2010) Early deficits in synaptic mitochondria in an Alzheimer's disease mouse model. Proc Natl Acad Sci USA 107:18670–18675.

Dumanis SB, Tesoriero JA, Babus LW, Nguyen MT, Trotter JH, Ladu MJ, Weeber EJ, Turner RS, Xu B, Rebeck GW, Hoe HS (2009) ApoE4 decreases spine density and dendritic complexity in cortical neurons *in vivo*. J Neurosci 29:15317–15322.

Dunkley PR, Jarvie PE, Robinson PJ (2008) A rapid Percoll gradient procedure for preparation of synaptosomes. Nat Protoc 3:1718–1728.

Flynn JM, Choi SW, Day NU, Gerencser AA, Hubbard A, Melov S (2011) Impaired spare respiratory capacity in cortical synaptosomes from Sod2 null mice. Free Radic Biol Med 50:866–873.

Gredilla R, Weissman L, Yang JL, Bohr VA, Stevnsner T (2012) Mitochondrial base excision repair in mouse synaptosomes during normal aging and in a model of Alzheimer's disease. Neurobiol Aging 33:694–707.

Gresack JE, Frick KM (2003) Male mice exhibit better spatial working and reference memory than females in a water-escape radial arm maze task. Brain Res 982:98–107.

Harold D et al. (2009) Genome-wide association study identifies variants at CLU and PICALM associated with Alzheimer's disease. Nat Genet 41:1088–1093.

Hinerfeld D, Traini MD, Weinberger RP, Cochran B, Doctrow SR, Harry J, Melov S (2004) Endogenous mitochondrial oxidative stress: neurodegeneration, proteomic analysis, specific respiratory chain defects, and efficacious antioxidant therapy in superoxide dismutase 2 null mice. J Neurochem 88:657–667.

Holtzman DM, Herz J, Bu G (2012) Apolipoprotein e and apolipoprotein e receptors: normal biology and roles in Alzheimer disease. Cold Spring Harb Perspect Med 2:a006312.

Ji Y, Gong Y, Gan W, Beach T, Holtzman DM, Wisniewski T (2003) Apolipoprotein E isoform-specific regulation of dendritic spine morphology in apolipoprotein E transgenic mice and Alzheimer's disease patients. Neuroscience 122:305–315.

Jofre-Monseny L, Minihane AM, Rimbach G (2008) Impact of apoE genotype on oxidative stress, inflammation and disease risk. Mol Nutr Food Res 52:131–145.

Kim J, Basak JM, Holtzman DM (2009) The role of apolipoprotein E in Alzheimer's disease. Neuron 63:287–303.

Kish SJ, Mastrogiacomo F, Guttman M, Furukawa Y, Taanman JW, Dozic S, Pandolfo M, Lamarche J, DiStefano L, Chang LJ (1999) Decreased brain protein levels of cytochrome oxidase subunits in Alzheimer's disease and in hereditary spinocerebellar ataxia disorders: a nonspecific change? J Neurochem 72:700–707.

Korwek KM, Trotter JH, Ladu MJ, Sullivan PM, Weeber EJ (2009) ApoE isoform-dependent changes in hippocampal synaptic function. Mol Neurodegener 4:21.

Kremer JR, Mastronarde DN, McIntosh JR (1996) Computer visualization of three-dimensional image data using IMOD. J Struct Biol 116:71–76.

Li KW, Jimenez CR (2008) Synapse proteomics: current status and quantitative applications. Expert Rev Proteomics 5:353–360.

Lin MT, Beal MF (2006) Mitochondrial dysfunction and oxidative stress in neurodegenerative diseases. Nature 443:787–795.

Mahley RW, Weisgraber KH, Huang Y (2009) Apolipoprotein E: structure determines function, from atherosclerosis to Alzheimer's disease to AIDS. J Lipid Res 50 (Suppl.):S183–188.

Massaad CA, Washington TM, Pautler RG, Klann E (2009) Overexpression of SOD-2 reduces hippocampal superoxide and prevents memory deficits in a mouse model of Alzheimer's disease. Proc Natl Acad Sci USA 106:13576–13581.

Moreira PI, Honda K, Liu Q, Santos MS, Oliveira CR, Aliev G, Nunomura A, Zhu X, Smith MA, Perry G (2005) Oxidative stress: the old enemy in Alzheimer's disease pathophysiology. Curr Alzheimer Res 2:403–408.

Mortensen EL, Hogh P (2001) A gender difference in the association between APOE genotype and age-related cognitive decline. Neurology 57:89–95.

Nathan BP, Barsukova AG, Shen F, McAsey M, Struble RG (2004) Oestrogen facilitates neurite extension via apolipoprotein E in cultured adult mouse cortical neurons. Endocrinology 145:3065–3073.

Nilsen J, Irwin RW, Gallaher TK, Brinton RD (2007) Oestradiol *in vivo* regulation of brain mitochondrial proteome. J Neurosci 27:14069–14077.

Numakawa T, Matsumoto T, Numakawa Y, Richards M, Yamawaki S, Kunugi H (2011) Protective action of neurotrophic factors and oestrogen against oxidative stress-mediated neurodegeneration. J Toxicol 2011:405194.

Ohkubo N, Mitsuda N, Tamatani M, Yamaguchi A, Lee YD, Ogihara T, Vitek MP, Tohyama M (2001) Apolipoprotein E4 stimulates cAMP response element-binding protein transcriptional activity through the extracellular signal-regulated kinase pathway. J Biol Chem 276:3046–3053.

Payami H, Zareparsi S, Montee KR, Sexton GJ, Kaye JA, Bird TD, Yu CE, Wijsman EM, Heston LL, Litt M, Schellenberg GD (1996) Gender difference in apolipoprotein E-associated risk for familial Alzheimer disease: a possible clue to the higher incidence of Alzheimer disease in women. Am J Hum Genet 58:803–811.

Petersen RC, Smith GE, Ivnik RJ, Tangalos EG, Schaid DJ, Thibodeau SN, Kokmen E, Waring SC, Kurland LT (1995) Apolipoprotein E status as a predictor of the development of

Alzheimer's disease in memory-impaired individuals. JAMA 273:1274–1278.

Postma A, Jager G, Kessels RP, Koppeschaar HP, van Honk J (2004) Sex differences for selective forms of spatial memory. Brain Cogn 54:24–34.

Raber J, Wong D, Yu GQ, Buttini M, Mahley RW, Pitas RE, Mucke L (2000) Apolipoprotein E and cognitive performance. Nature 404:352–354.

Radyuk SN, Michalak K, Klichko VI, Benes J, Rebrin I, Sohal RS, Orr WC (2009) Peroxiredoxin 5 confers protection against oxidative stress and apoptosis and also promotes longevity in Drosophila. Biochem J 419:437–445.

Rahman I, Kode A, Biswas SK (2006) Assay for quantitative determination of glutathione and glutathione disulfide levels using enzymatic recycling method. Nat Protoc 1:3159–3165.

Schrimpf SP, Meskenaite V, Brunner E, Rutishauser D, Walther P, Eng J, Aebersold R, Sonderegger P (2005) Proteomic analysis of synaptosomes using isotope-coded affinity tags and mass spectrometry. Proteomics 5:2531–2541.

Singh M, Dykens JA, Simpkins JW (2006) Novel mechanisms for oestrogen-induced neuroprotection. Exp Biol Med (Maywood) 231:514–521.

Stone DJ, Rozovsky I, Morgan TE, Anderson CP, Finch CE (1998) Increased synaptic sprouting in response to oestrogen via an apolipoprotein E-dependent mechanism: implications for Alzheimer's disease. J Neurosci 18:3180–3185.

Sun Y, Wu S, Bu G, Onifade MK, Patel SN, LaDu MJ, Fagan AM, Holtzman DM (1998) Glial fibrillary acidic protein-apolipoprotein E (apoE) transgenic mice: astrocyte-specific expression and differing biological effects of astrocyte-secreted apoE3 and apoE4 lipoproteins. J Neurosci 18:3261–3272.

Sun ZW, Zhu YX, Liu HY, Liu J, Zhu XQ, Zhou JN, Liu RY (2007) Decreased cerebral blood flow velocity in apolipoprotein E epsilon4 allele carriers with mild cognitive impairment. Eur J Neurol 14:150–155.

Valla J, Yaari R, Wolf AB, Kusne Y, Beach TG, Roher AE, Corneveaux JJ, Huentelman MJ, Caselli RJ, Reiman EM (2010) Reduced posterior cingulate mitochondrial activity in expired young adult carriers of the APOE epsilon4 allele, the major late-onset Alzheimer's susceptibility gene. J Alzheimers Dis 22:307–313.

Wang QS, Tian L, Huang YL, Qin S, He LQ, Zhou JN (2002) Olfactory identification and apolipoprotein E epsilon 4 allele in mild cognitive impairment. Brain Res 951:77–81.

Whittaker VP (1993) Thirty years of synaptosome research. J Neurocytol 22:735–742.

Whittaker VP, Michaelson IA, Kirkland RJ (1964) The separation of synaptic vesicles from nerve-ending particles ('synaptosomes'). Biochem J 90:293–303.

Wickelgren I (1997) Oestrogen stakes claim to cognition. Science 276:675–678.

Xu PT, Li YJ, Qin XJ, Scherzer CR, Xu H, Schmechel DE, Hulette CM, Ervin J, Gullans SR, Haines J, Pericak-Vance MA, Gilbert JR (2006) Differences in apolipoprotein E3/3 and E4/4 allele-specific gene expression in hippocampus in Alzheimer disease. Neurobiol Dis 21:256–275.

Yaffe K, Haan M, Byers A, Tangen C, Kuller L (2000) Oestrogen use, APOE, and cognitive decline: evidence of gene-environment interaction. Neurology 54:1949–1954.

Yang SY, He XY, Schulz H (2005) Multiple functions of type 10 17beta-hydroxysteroid dehydrogenase. Trends Endocrinol Metab 16:167–175.

Yue X, Lu M, Lancaster T, Cao P, Honda S, Staufenbiel M, Harada N, Zhong Z, Shen Y, Li R (2005) Brain oestrogen deficiency accelerates Abeta plaque formation in an Alzheimer's disease animal model. Proc Natl Acad Sci USA 102:19198–19203.

Zhang LF, Shi L, Liu H, Meng FT, Liu YJ, Wu HM, Du X, Zhou JN (2011) Increased hippocampal tau phosphorylation and axonal mitochondrial transport in a mouse model of chronic stress. Int J Neuropsychopharmacol 15:1–12.